

# Improving the Performance of Variable Data Rate Architectures for Optical LEO Direct-to-Earth Links

Bertold Ian Bitachon<sup>1</sup>, Michael Baumann<sup>1</sup>, Johannes Widmer<sup>2</sup>, Michal Kuklewski<sup>2</sup>, Hannah Lindberg<sup>2</sup>,  
Mathieu Berges<sup>2</sup>, Juerg Leuthold<sup>1</sup>

*Institute of Electromagnetic Fields (IEF), ETH Zurich, Gloriastrasse 35, 8092 Zurich, Switzerland*  
*Thales Alenia Space Switzerland, Schaffhauserstrasse 580, Zürich 8052, Switzerland*  
Author e-mail address: bertold.bitachon@ief.ee.ethz.ch

**Abstract:** Usage of new spreading factors is shown to improve the rate granularity, performance and photon efficiency of variable data rate architectures intended for optical low earth orbits to earth links. © 2022 The Author(s)

## 1. Introduction

In recent years, optical communication has increasingly penetrated satellite communication intended for low earth orbit (LEO) to deep space communications. For LEO applications interests are in establishing new direct-to-Earth (DTE) optical communication links, for acquiring high resolution earth observation, or the operation of in-orbit datacenters [1]. However, LEO-DTE links are not without challenges. One of the major challenges for this channel is the power variability during a satellite pass.

Fig. 1 depicts an illustration of a typical LEO satellite pass and its received power profile. The received power varies as a function of elevation angle  $\theta$ , with the maximum received power at  $90^\circ$  of elevation. Current and planned optical LEO-DTE systems transmit at a constant data rate during the satellite pass [2]. Therefore, a trade-off must be taken between a high data rate and a long transmission window. High data rate requires a favorable channel condition located at high elevation angle, while a long transmission window requires a transmission at low angle implying a low data rate. The obvious solution to this dilemma is a variable data rate, where different rates are transmitted during the pass.

The idea of variable data rate (VDR) is to split the pass into predefined set of sectors where the transmitter transmits at a predefined rate in each sector, see Fig. 1(b). Within the ongoing Consultative Committee for Space Data Systems (CCSDS) standardization of the optical LEO-DTE physical layer, referred to as O3K [3, 4] throughout this text, the rate variability is achieved by spreading the data bit by a spreading factor (SF) to the highest possible rate that either the transmitter or the receiver can support. In [4] it was shown that for a single bit spreading, repetition coding with a spreading factor (SF) is the optimum spreading. For example, in a SF = 4,

$$s(b) = \begin{cases} [0, 0, 0, 0]^T, & b = 0 \\ [1, 1, 1, 1]^T, & b = 1 \end{cases} \quad (1)$$

where  $s(b)$  is the transmitted sequence for input bit  $b$ . Using this function, the data rate can be lowered by factor of SF. Although the spreading is simple in hardware, the supported rates are rather limited ( $SF \in \{1, 2, 4, 8, 16\}$  for O3K [3]), therefore the total throughput is also limited during the pass.

In this paper, we propose an extension to the VDR of the O3K standard that increases the rate granularity and by this the total throughput during a satellite pass. We also show that in some cases, the proposed spreading factors outperform the O3K standard in term of performance and energy efficiency. The new spreading factors are based on spreading multiple bits at a time instead of one bit.

## 2. Variable Data Rate Extension

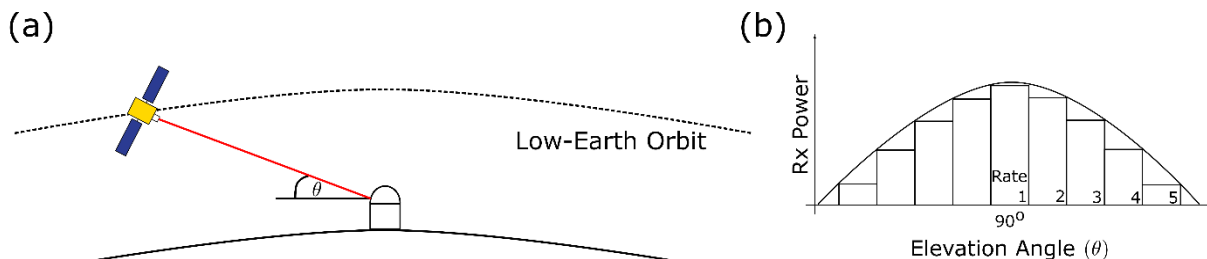


Fig. 1. (a) Illustration of a low-earth orbit satellite pass. (b) Received power profile as function of elevation angle ( $\theta$ ) and variable data rate scheme.

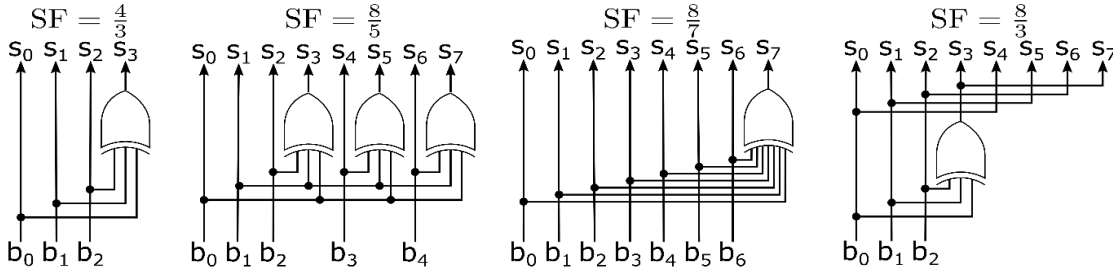


Fig. 3. Hardware implementation for the proposed spreading factor 4/3, 8/5, 8/7, and 8/3. Higher spreading factors are achieved by a repetition of lower spreading factor until the numerator meets one of the spreading factors of O3K.

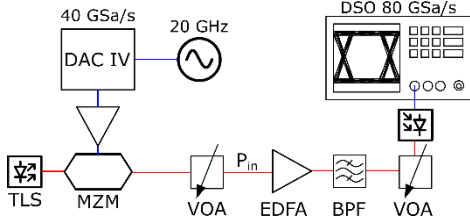


Fig. 2. Experimental setup for direct-detection transmission.

The new spreading factors are based on a multidimensional set partitioning (SP) scheme [5]. In 4- or 8-dimensional (D) space, we have either 16 or 256 possible spread sequences. We then select a subset of 8 sequences from the 4D space and a subset of 128 and 32 sequences form the 8D space. The selection was done by successively increasing the minimum hamming distance between the sequences. Fig. 3 depicts the hardware implementation of the proposed new spreading methods employing simple multiple input XOR gates. To start, we begin with some basic parity schemes such as the ones with SF = 4/3, 5/8 or 8/7. To increase the spreading even further one may repeat the basic sequence until the numerator

meets one of the spreading factors of O3K ( $SF \in \{1,2,4,8,16\}$ ). For instance, SF = 8/3 in Fig. 3 is obtained by repeating the SF=4/3 twice. For decoding, we calculate the log likelihood ratio of each transmitted bit using the received symbols.

We then tested the proposed method in a fiber-based experiment. Fig. 2 shows the experimental setup. We generated the 10 Gbit/s electrical signal using a DAC IV by Micram running at 40 GSa/s. It should be noted that we also scrambled the spread sequence within the transmitter DSP before transmission. A Mach-Zehnder modulator (MZM) with 3 dB bandwidth of 15 GHz was then used to transfer the electrical signal to a 1550 nm carrier. We then varied the received optical power ( $P_{in}$ ) into a pre-amplified receiver (EDFA with PIN). The PIN-based receiver has a 3 dB bandwidth of 70 GHz. We then digitized the received electrical signal using an 80 GSa/s oscilloscope followed by offline DSP consisting of timing recovery, and T-spaced feedforward equalizer.

### 3. Results and Discussion

Fig. 4(a) shows the BER as a function of the received power for different spreading factors while Fig. 4(b) shows the normalized GMI (NGMI) as a function of received power for different spreading factors. Fig. 4 shows that we have increased the rate granularity of our transmission since the performance of our proposed method is located in between

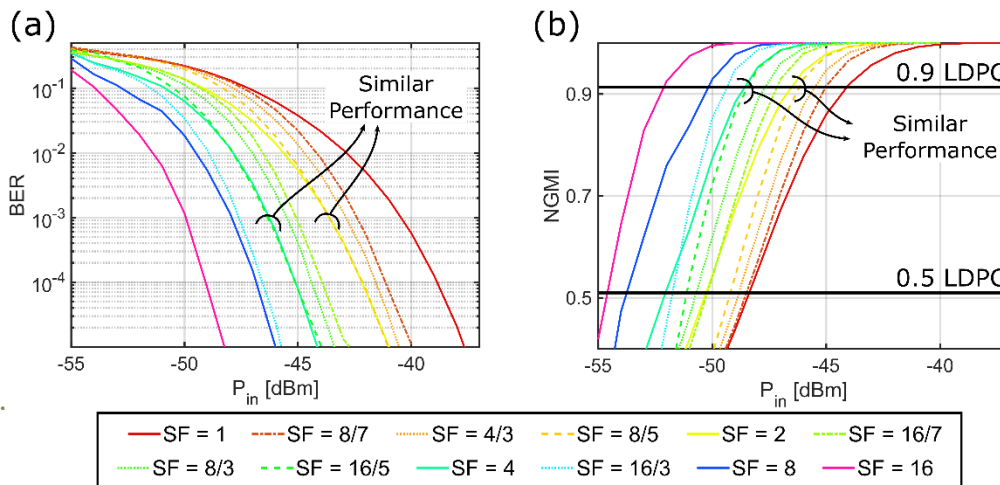


Fig. 4. (a) Measured BER as a function of the received power to the pre-amplified receiver for different spreading factors. (b) NGMI as a function of the received power to the pre-amplified receiver for different spreading factors.

the BER and NGMI curve of the O3K standard (solid lines). We also mark the NGMI threshold for the LDPC code of the O3K with code rate of 0.5 and 0.9 [3]. The NGMI threshold is based on numerical simulation. It can be seen that the rate granularity is finer at code rate of 0.9 than that of code rate 0.5 this is because the minimum hamming distance is not high enough for very low power operation. It can also be seen that at a code rate of 0.9, the spreading factors of 8/5 and 16/5 have almost similar performance to the O3K standard with spreading factor of 2 and 4, respectively (see encircled plots in Fig. 4). Showing that the new parity schemes offer higher throughput for a negligible received power penalty.

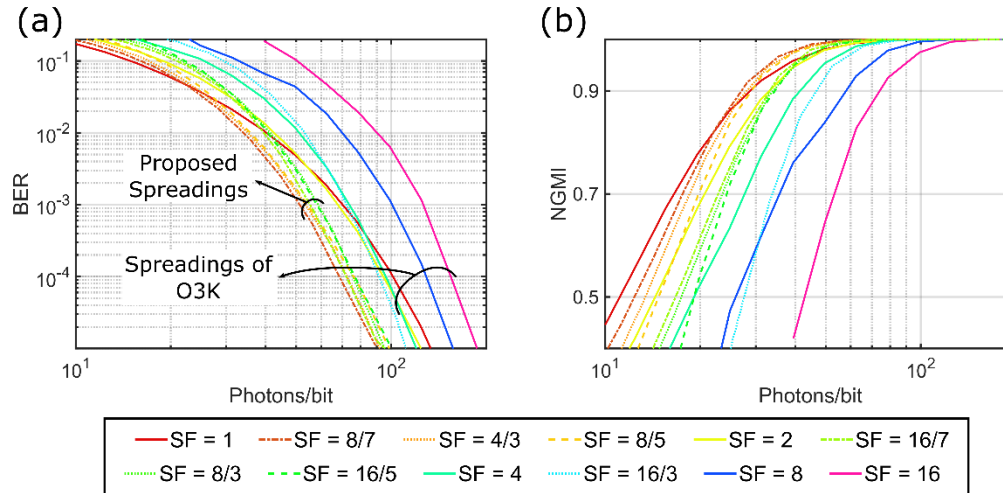


Fig. 5. (a) BER as a function of the number of photons per bit for different spreading factors. (b) NGMI as a function of the received power to the pre-amplified receiver for different spreading factors.

To understand the energy efficiency of the proposed spreading factors, we plot the BER as a function of photons per bit in Fig. 5(a) and the NGMI as a function of photons per bit in Fig. 5(b). Fig. 5(a) and (b) show that at high received power, the majority of our proposed spreading factors are more efficient than those of the O3K standard (see encircled plots) while at low received power most of our proposed spreading factors are more efficient than most of the O3K standard, except the one with spreading 1. Furthermore, Fig. 5 shows how the solid plots get closer at high photon/bit numbers. This is because the spreading factor can be traded in against a lower average power, where the photons/bit number remains constant. But at low received powers, the spreading of the O3K standard diverges. This is because at high received powers we are shot noise limited so that by doubling the spreading factor (halving the rate), the required power can be reduced by factor 2 as well – and thus, the photon per bit stays the same. As the received power decreases, we are more limited by the thermal noise so that doubling the spreading factor lowers the power requirement by a factor of  $\sqrt{2}$  thus increasing the number of photons per bit by  $\sqrt{2}$ . Fig. 5 shows that the standard O3K can operate at low power, but not efficient. However, most of our proposed spreading factors are effective in both at low and high received power situations.

#### 4. Conclusion

We propose several new spreading factors as a compliment to the intended variable data rate (VDR) scheme of the ongoing O3K standardization. The proposed spreading factors are based on set partitioning and repetition. We show that the proposed spreading factors not only increase the rate granularity of the VDR scheme but also, in some cases, outperforms the O3K standard both in term of performance and energy efficiency.

#### Acknowledgement

This project is supported by ESA project Variable-data-rate transmitter for LEO direct-to-Earth optical links (VARTO).

#### References

- [1] S. Müncheberg *et al.*, "Development status and breadboard results of a laser communication terminal for large LEO constellations," ICSO 2019.
- [2] C. Fuchs *et al.*, "OSIRISv1 on Flying Laptop: Measurement Results and Outlook," IEEE ICSOS 2019.
- [3] *Pink Sheets for Optical Communications Coding and Synchronization*, 142.0-B-1, June 2022.
- [4] P. D. Arapoglou *et al.*, "Variable Data Rate Architectures in Optical LEO Direct-to-Earth Links: Design Aspects and System Analysis," *JLT*, 2022.
- [5] J. Renaudier *et al.*, "Experimental transmission of Nyquist pulse shaped 4-D coded modulation using dual polarization 16QAM set-partitioning schemes at 28 Gbaud," OFC 2013.